

AN OSCILLATOR MODEL FOR HIGH-PRECISION SYNCHRONIZATION PROTOCOL DISCRETE EVENT SIMULATION

Georg Gaderer
Austrian Academy of Sciences
Viktor Kaplan Straße 2, A-2700 Wiener Neustadt, Austria
E-mail: *georg.gaderer@oeaw.ac.at*

Patrick Loschmidt, Anetta Nagy, Roman Beigelbeck, Jörgen Mad
Austrian Academy of Sciences
{*Patrick.Loschmidt, Anetta.Nagy, Roman.Beigelbeck, Joergen.Mad*}
@oeaw.ac.at

Nikolaus Kerö
Oregano Systems
keroe@oregano.at

Abstract

It is well known that a common notion of time in distributed systems can be used to ensure additional properties such as real-time behavior or the identification of the order of events. As large-scale hardware testbeds for such systems are neither efficient nor easy to manage, discrete event simulations (DES) can be used to model such networks. However, to ensure an exact behavior of such simulations, high precise models of the local clocks are also needed: the driving oscillators have to be modeled in a way that a DES simulation of a free-running node clock shows the same Allan deviation as the simulated counterpart. This paper shows an approach to find a corresponding model for a simulator using white noise and a filter with the same power density spectrum as real-world oscillators.

INTRODUCTION

The advantage of synchronized clocks for network nodes is very well known. One of the most popular applications is time division multiple access (TDMA) on shared media and the direct use for real-time tasks. Besides that, the simple need for the capability of sequential ordering of events occurring in large distributed systems [1] depends on synchronized clocks. Standards like the upcoming IEEE 1588 protocol allow the synchronization of clocks over packet-oriented networks.

In such commercial or industrial environments, the number of nodes often reaches a number of hundred or more. Consequently, for design and development of control loops, devices or even enhancements of

protocols, the implementation of prototype testbeds is neither cost efficient nor trivial to manage. Thus, there is a need for simulation of the operation and performance of such large systems.

Besides the cost-efficient implementation of a simulation for large-scale networks, it is possible to run simulations faster or slower than in real time¹, which opens new possibilities to verify effects that are too difficult to see in hardware-based testbeds. Finally, simulation of timely behavior of geographically distributed elements has the advantage of having a common notion of real time available at each and every node. Such fully synchronized clocks at every node can, of course, not replace the actual notion of time at a node (which is, of course, influenced by the local clock and, therefore, in general different at each and every node).

The remainder of this paper is structured as follows: after an introduction into the problems of discrete event simulation, the theory of power density spectra of oscillators will be given. This will be followed by an example of parameter extraction of a commercial off-the-shelf oscillator and a conclusion, as well as an outlook for further work.

DISCRETE EVENT SIMULATORS

In general, two possibilities for the simulation of time-driven systems exist:

- Continuous time simulators, where a timescale is cut into arbitrary small parts and the status of the system is fully determined at each and every microtick of the simulator. However, for the case of high-precision clock synchronization, this turns out to be neither efficient nor manageable with today's reasonably available computing power.
- Discrete event Simulation (DES). This class of simulators is built on events, which can be raised at a certain, so-called simulation time. This simulation time is a global equally spaced timescale, such as TAI. The main advantage comes from the fact that the simulator keeps track on all upcoming events and their occurrence, which allows the system to "jump" from one event to the next. The time in between is not simulated and, therefore, skipped out, which increases the performance dramatically.

When using DES for simulating networks performing clock synchronization, each simulated node has to use its own notion of time and not the globally available (and, therefore, evidently synchronized) simulation time. The task of translating this simulation-wide identical time notion into a node-specific one is done by oscillator models, which are the actual topic of this investigation.

The obviously most simplistic approach is to model an oscillator with a drifting frequency offset. Although this model has shown to be very useful, such a jitter-less approach turns out not to be enough precise for simulation scenarios where clock synchronization in the sub-nanosecond range is needed. Due to the fact that external events might also trigger a simulated node to wake up and take action, it cannot be assumed that there is no earlier run (externally inserted new event) than the locally calculated next event for a node.

PROBLEM STATEMENT

This non-continuous progress in time requires special handling in the implementation of an oscillator

¹ In this paper, the notation real-time shall address the behavior of a system to react within guaranteed (timely) deadlines, whereas real time will be used to indicate a physical timescale such as TAI.

model. This means that any oscillator has to store the upcoming future of his scheduled tick events, in order to produce timely consistent output in case of an event insertion (in the order before already scheduled events).

The problem with the simple drifting frequency model is, besides the poor mapping of physical effects like aging, that noise and statistical effects are not covered. Consequently, an oscillator model, which gives a more realistic view of the reality, is needed.

While the determination of the next event is easy when using a non-statistical behavior, an appropriate noise generator is required as base for calculating statistical properties. Common simulators provide random number generators for white noise. The goal for the design of the presented model is to develop a filter structure, which filters white noise in a way that the Allan deviation of real and modeled oscillators match. In order to obtain the necessary parameters for the construction of a matching model, the power density spectrum and the setup for measuring a quartz crystal oscillator is used. After extracting the required parameters (bandwidth, border frequencies, and the corner frequencies) from the measurement, the mathematical construction of the filter completes the development process.

OSCILLATOR MODEL

The Allan variance [2] σ_y^2 of a power density spectrum $S_y(f)$ limited to $[f_{lc}, f_{uc}]$ is defined by:

$$\sigma_y^2(\tau, f_{lc}, f_{uc}) := 2 \int_{f_{lc}}^{f_{uc}} \frac{\sin^4(\pi f \tau)}{(\pi f \tau)^2} S_y(f) df. \quad (1)$$

It is well known [3] that a model of the power density spectrum of an oscillator is given by:

$$S_{y,i}(f) = \begin{cases} h_i f^i & f_{lc} \leq f \leq f_{uc} \\ 0 & \text{otherwise} \end{cases} \quad (2)$$

with $S_y(f) = \sum S_{y,i}(f)$ with $-2 \leq i \leq 2$. Using this equation, the contributing parts of the Allan variance $\sigma_{y,i}^2$ can be defined as:

$$\sigma_{y,i}^2(\tau; f_{lc}, f_{uc}) := 2 \int_{f_{lc}}^{f_{uc}} \frac{\sin^4(\pi f \tau)}{(\pi f \tau)^2} S_{y,i}(f) df \quad (3)$$

with the trivial relationship:

$$\sigma_y^2(\tau; f_{lc}, f_{uc}) = \sum_{i=-2}^2 \sigma_{y,i}^2(\tau; f_{lc}, f_{uc}). \quad (4)$$

A filter with a pulse response that satisfies this equation will respond to white noise with an output having the same Allan deviation as the measured system. However, the evaluation of the above equations for $f_{lc} \rightarrow 0$ and $f_{uc} \rightarrow \infty$ deliver meaningful results only for values of $i = \{-2, -1, 0\}$, whereas the parts for 1 and 2 reveal infinite results for the integral.

This fact is well known, as Jacques Rutman wrote in *Characterization of Frequency Stability in Precision Frequency Sources* [4]: “It is necessary to specify the value and shape of the low-pass filter for noise types with $i > 0$. Most common shapes are the infinitely sharp low-pass filter ...”

Nevertheless, for values of $f_{uc} < \infty$, a solution of the integrals can be given with the help of the definition of the sine integral:

$$S(\zeta) := \int_0^\zeta \frac{\sin(u)}{u} du \quad (5)$$

and cosine integral:

$$C(\zeta) := \gamma + \ln(\zeta) + \int_0^\zeta \frac{\cos(u)-1}{u} du = -\int_\zeta^\infty \frac{\cos(u)}{u} du \quad (6)$$

[5], as well as the Euler-Mascheroni Constant $\gamma \approx 0.577$ [6], one can find new solutions of the contributory parts of the Allan deviation after a short calculation.

$$\sigma_{y,-2}^2(\tau; 0, f_c) = \pi\tau \left\{ \frac{8S(4u_g) - 4S(2u_g)}{3} - \frac{\sin^2(u_g) [4u_g^2 + 2u_g \sin(2u_g) + (8u_g - 1) \cos(2u_g) + 1]}{3u_g^3} \right\} h_{-2}, \quad (7e)$$

$$\sigma_{y,-1}^2(\tau; 0, f_c) = \left\{ \ln(4) + 2C(2u_g) - 2C(4u_g) - \frac{[4u_g \cos(u_g) + \sin(u_g)] \sin^3(u_g)}{u_g^2} \right\} h_{-1}, \quad (7b)$$

$$\sigma_{y,0}^2(\tau; 0, f_c) = \frac{1}{\pi\tau} \left\{ 2S(2u_g) - S(4u_g) - \frac{\sin^4(u_g)}{u_g} \right\} h_0, \quad (7c)$$

$$\sigma_{y,1}^2(\tau; 0, f_c) = \frac{1}{(\pi\tau)^2} \left\{ \frac{\ln(4) + 3\gamma + 3\ln(u_g) + C(4u_g) - 4C(2u_g)}{4} \right\} h_1, \quad (7d)$$

$$\sigma_{y,2}^2(\tau; 0, f_c) = \frac{1}{(\pi\tau)^3} \frac{12u_g + \sin(4u_g) - 8\sin(2u_g)}{16} h_2 \quad (7e)$$

with the substitution $u_c(\tau) = \pi f_c \tau$. Finally, the actual values can be calculated with

$$\sigma_{y,i}^2(\tau; f_{lc}, f_{uc}) = \sigma_{y,i}^2(\tau; 0, f_{uc}) - \sigma_{y,i}^2(\tau; 0, f_{lc}). \quad (8)$$

With these equations, it can be seen that the parts for $i = -2, -1$, and 0 are independent of f_c , in the case of $u_g \gg 1$. Moreover, for $i=1$ and 2 , the respective parts of the Allan deviation approach infinity with growing numbers of f_c .

PARAMETER EXTRACTION FROM MEASURED ALLAN DEVIATIONS

The parameter extraction now can be done very easily with the following approach:

- 1.) The values of $\sigma_{y,1}^2$ and $\sigma_{y,2}^2$ are limited by the test setup. With that limitation, the lower and the upper cut-off frequency, which are defined by the measurement equipment, can be defined. Moreover, the relationship $2 \pi f_{uc} \tau \gg 1$ should be satisfied all relevant values of τ .
- 2.) The graphical curve of σ_y^2 is measured empirically.
- 3.) The theoretical values of the variances (in multiples of h_i) have to be determined via equation (7).

- 4.) The values of h_i get determined numerically with the method of the infinity norm $\| \cdot \|_{\infty}$.

With that parameters the power density spectrum of $S_y(f)$ is sufficiently determined, and can be used for a filter design.

OSCILLATOR CHARACTERIZATION

As the study of the long-term stability of an oscillator is rather time consuming, it is desirable to make a measurement setup that will perform the entire measurement automatically. For this reason, a measurement environment was set up as depicted in Figure 1. A central part is the SR620 Universal Time-Interval Counter [7]. This device plays two roles: on the one hand, it is responsible for the measurement of the period of the oscillator under test, multiple periods respectively. On the other hand, it is used as a remote control for the FPGA board. This board is used as a frequency divider and provides the counter with a range of frequencies based on the temperature-stabilized oscillator under test. In order to cancel out the influence of clock uncertainties originating from device internal oscillators, the SR620 device was driven by a stable rubidium frequency standard. The overall measurement is controlled by a PC, which also stores the measurement results.

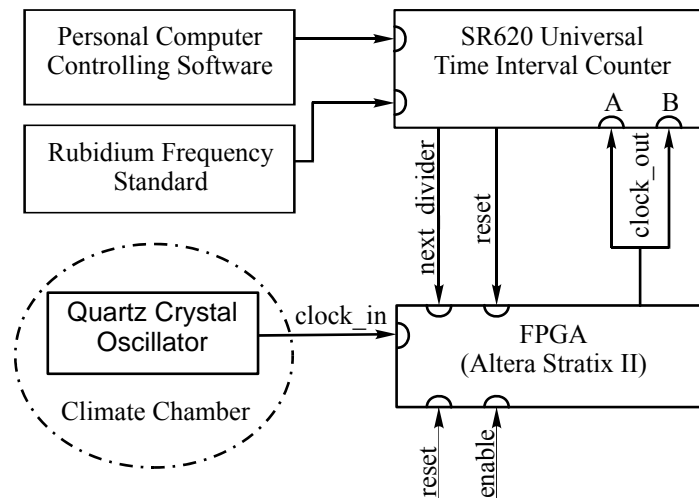


Figure 1. Measurement setup.

MEASUREMENT ACQUISITION

To demonstrate the described modeling approach, the Allan variance of a 2 MHz oscillator was determined. This was done by taking samples using different averaging times of the oscillator with the help of the measuring setup described in the previous section. The range of τ was chosen to be set to logarithmic equally spaced values 1 μ s to 500 s. This upper value of τ is determined by measurement equipment. Now the Allan variance can be calculated by [8]:

$$\sigma_y^2 = \frac{1}{2(N-1)} \sum_{n=1}^{N-1} (y_{n+1} - y_n)^2 \quad (9)$$

where y_n is the normalized frequency departure defined as:

$$y_n = \frac{(x_{n+1} - x_n)}{\tau} \quad (10)$$

where x_n (the so-called time errors) are the measured samples and N is the number of samples. After calculating the results, the Allan variance versus τ is displayed on a double logarithmic plot.

The next step is to calculate the values of the h_i parameters. Although the structure of the model (2) suggests the straightforward approach of choosing five measured values and the solution of the resulting linear equation system, this turns out not to be the optimal approach. The latter is caused by the fact that, in general, imperfections such as noise will not lead to an optimal fit. That is why an approximation of the Allan variance and the parameters of (2) are needed. This function needs to be in form of equation (4). The approximation can be done in several ways, although not all of them have shown to be successful in the general case. Using the methods of the least quadratic error does not prove to be very successful, as the logarithmic and, therefore, not equally spaced measurements and the relatively big range of measurement values do not lead to an optimal convergence. However, instead of using the sum of the quadratic error, or $\| \cdot \|_2$, the infinity norm $\| \cdot \|_\infty$ of the error vector was used. However, the success this method heavily depends on the starting values of this unconstrained, nonlinear approximation; a first rough guess of these values can be obtained using the least quadratic error method.

Figure 2 shows the Allan variance as a function of τ displayed on a double logarithmic plot for two cases: the red-marked squares have been determined by measurement, and the blue curve represents the approximation using these points.

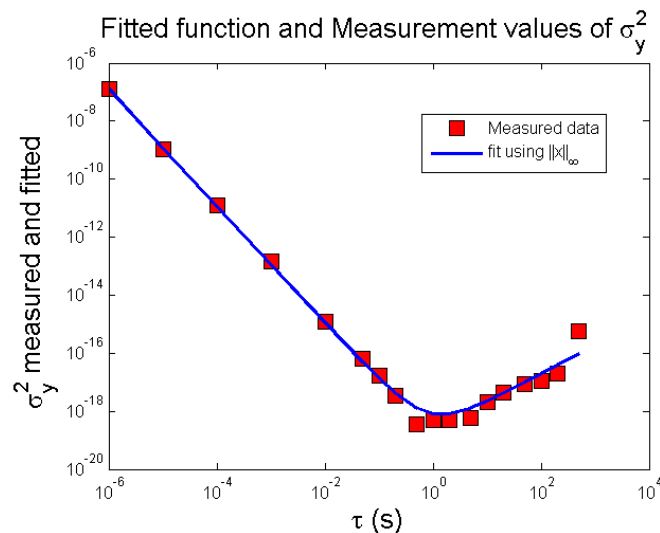


Figure 2. The Allan variance plot of the real oscillator and of the approximation.

Since the approximated function has the form of:

$$\sigma_y^2 = 10^{-18} \cdot (0.18974971293808\tau + 0.28527328756472 + 0.22711027708165\tau^{-1} + 0.10828422348094\tau^{-2} + 0.00000002073475\tau^{-3}) \quad (11)$$

The h_i parameters can be easily calculated with equation (7). The calculated values of the h_i parameters are illustrated in Table 1.

Table 1. The values of the h_i parameters.

i	Value
-2	$1.2846933726509597 \cdot 10^{-20}$
-1	$2.0580462073483913 \cdot 10^{-19}$
0	$4.542215104500719 \cdot 10^{-19}$
1	$5.2216853435436694 \cdot 10^{-20}$
2	$5.2216853435436694 \cdot 10^{-20}$

CONCLUSION AND FURTHER WORK

For discrete event simulations of high-precision clock synchronization, a proper simulation model of oscillators is more than important. In fact a model, also covering statistical behavior such as jitter, and not only an aging frequency offset, is mandatory. This turns out to be not too easy, as it has to be possible to recall the simulator model several times, but no output value must be inconsistent with a previous answer of the simulation. Such a model can be built via filtering a white-noise source with a filter that provides the same Allan deviation as a real-world oscillator. This paper explains how to extract those parameters of actual measurements using the infinity norm $\| \cdot \|_{\infty}$ method. This leads to the parameters of the spectral power density that can be used as a basis for the filter design. This approach is demonstrated with some real-world measurements of an oscillator.

As a next step, this model of the power density spectrum will be estimated by a pink-noise filter, and more and deeper investigations concerning measurement-model fitting will be done.

ACKNOWLEDGMENTS

The authors wish to thank Mrs. Sigrid Seiser for many useful hints and her help assembling this paper.

REFERENCES

- [1] L. Lamport, 1987, "Time, Clocks, and the Ordering of Events in a Distributed System," *Communications of the ACM*, **21**, 558-565.

- [2] D. W. Allan, 1986, “*Time and Frequency (Time-Domain) Characterization, Estimation, and Prediction of Precision Clocks and Oscillators,*” **IEEE Transactions on Ultrasonics, Ferroelectrics and Frequency Control**, UFFC-34, 647-654.
- [3] E. Rubiola, 2005, “*The Leeson Effect–Phase Noise in Quasilinear Oscillators,*” <http://arkiv.org/abs/physics/0502143>
- [4] J. Rutman and F. L. Walls, 1991, “*Characterization of Frequency Stability in Precision Frequency Sources,*” **Proceedings of the IEEE**, 79, 952-960.
- [5] M. Abramowitz and I. A. Stegun, 1972, **Handbook of Mathematical Functions with Formulas, Graphs, and Mathematical Tables**, 9th printing (Dover, New York), pp. 231-233.
- [6] S. R. Finch, 2003, **Mathematical Constants** (Cambridge University Press, Cambridge, England), pp. 28-40.
- [7] Stanford Research Systems, 1989, “*MODEL SR620 Universal Time Interval Counter,*” Stanford Research Systems, Rev. 2.7 (2/2007).
- [8] D. W. Allan, N. Ashby, and C. C. Hodge, 1997, “*The Science of Timekeeping,*” Hewlett-Packard Application Note 1289.